Quantifying the impact of proximity error correction on plasmonic metasurfaces [Invited]

Sebastian A. Schulz,[1,*] Jeremy Upham,[1] Frédéric Bouchard,[1] Israel De Leon,[1] Ebrahim Karimi[1] and Robert W. Boyd[1,2]

[1] *Department of Physics, University of Ottawa, 25 Templeton Street, Ottawa, K1N6N5, Canada*
[2] *Institute of Optics and Department of Physics and Astronomy, University of Rochester, 275 Hutchison Rd., Rochester, NY 14627, USA*
[*] *sschulz@uottawa.ca*

Abstract: Plasmonic metasurfaces are often limited in their application by poor device performance, which is caused - in part - by deviations between fabricated devices and the ideal design. We show in this letter that these deviations are reduced significantly by shape-correction, intra-structure proximity error correction. We show experimentally that the fabrication fidelity alone is not a good indicator of the device quality and that direct measurements of the optical performance are necessary. Our fabrication improvements result in increased optical performance, reaching a measurement fidelity as high as 90%.

OCIS codes: (110.4235) Nanolithography; (160.3918) Metamaterials; (220.4241) Nanostructure fabrication; (250.5403) Plasmonics.

References and links

1. N. Yu, P. Genevet, M. A. Kats, F. Aieta, J.-P. Tetienne, F. Capasso, and Z. Gaburro, "Light propagation with phase discontinuities: generalized laws of reflection and refraction," Science **334**(6054), 333–337 (2011).
2. A. V. Kildishev, A. Boltasseva, and V. M. Shalaev, "Planar photonics with metasurfaces," Science **339**(6125), 1232009 (2013).
3. I. De Leon, M. J. Horton, S. A. Schulz, J. Upham, P. Banzer and R. W. Boyd "Strong, spectrally-tunable chirality in diffractive metasurfaces," accepted for publication in Scientific Reports (2015).
4. N. Lawrence, J. Trevino, and L. Dal Negro, "Control of optical orbital angular momentum by Vogel spiral arrays of metallic nanoparticles," Opt. Lett. **37**(24), 5076–5078 (2012).
5. N. Yu and F. Capasso, "Flat optics with designer metasurfaces," Nat. Mater. **13**(2), 139–150 (2014).
6. A. Arbabi, Y. Horie, M. Bagheri, and A. Faraon, "Complete Control of Polarization and Phase of Light with High Efficiency and Sub-wavelength Spatial Resolution,"arXiv:1411.1494 [physics.optics], Faraon (2014).
7. F. Aieta, P. Genevet, M. A. Kats, N. Yu, R. Blanchard, Z. Gaburro, and F. Capasso, "Aberration-Free Ultrathin Flat Lenses and Axicons at Telecom Wavelengths Based on Plasmonic Metasurfaces," Nano Lett. **12**(9), 4932–4936 (2012).
8. Z. Bomzon, G. Biener, V. Kleiner, and E. Hasman, "Space-variant Pancharatnam-Berry phase optical elements with computer-generated subwavelength gratings," Opt. Lett. **27**(13), 1141–1143 (2002).
9. E. Karimi, S. A. Schulz, I. De Leon, H. Qassim, J. Upham, and R. W. Boyd, "Generating optical orbital angular momentum at visible wavelengths using a plasmonic metasurface," Light Sci. Appl. **3**(5), e167 (2014).
10. F. Bouchard, I. De Leon, S. A. Schulz, J. Upham, E. Karimi, and R. W. Boyd, "Optical spin-to-orbital angular momentum conversion in ultra-thin metasurfaces with arbitrary topological charges," Appl. Phys. Lett. **105**(10), 101905 (2014).
11. J. Lin, P. Genevet, M. A. Kats, N. Antoniou, and F. Capasso, "Nanostructured Holograms for Broadband Manipulation of Vector Beams," Nano Lett. **13**(9), 4269–4274 (2013).
12. L.-J. Black, Y. Wang, C. H. de Groot, A. Arbouet, and O. L. Muskens, "Optimal Polarization Conversion in Coupled Dimer Plasmonic Nanoantennas for Metasurfaces," ACS Nano **8**(6), 6390–6399 (2014).
13. G. V. Naik, J. L. Schroeder, X. Ni, A. V. Kildishev, T. D. Sands, and A. Boltasseva, "Titanium nitride as a plasmonic material for visible and near-infrared wavelengths," Opt. Mater. Express **2**(4), 478–489 (2012).
14. K. M. McPeak, S. V. Jayanti, S. J. P. Kress, S. Meyer, S. Iotti, A. Rossinelli, and D. J. Norris, "Plasmonic Films Can Easily Be Better: Rules and Recipes," ACS Photonics **2**(3), 326–333 (2015).
15. J. S. Greeneich and T. Van Duzer, "An exposure model for electron-sensitive resists," IEEE Trans. Electron. Dev. **21**(5), 286–299 (1974).
16. P. Rai-Choudhury, *Handbook of Microlithogaphy, Micromachining, and Microfabrication. Volume 1: Micorlithogarphy* (SPIE Press, 1997).
17. M. Parikh, "Corrections to proximity effects in electron beam lithography, I. Theory," J. Appl. Phys. **50**(6), 4371 (1979).

#248011 Received 17 Aug 2015; revised 1 Oct 2015; accepted 26 Oct 2015; published 10 Nov 2015

Corrected: 24 November 2015

18. C. S. Ea and A. D. Brown, “Incorporating a corner correction scheme into enhanced pattern area density proximity effect correction,” J. Vac. Sci. Technol. B **19**(5), 1985 (2001).
19. T. Kimpel, M. Schulz, R. Zimmermann, H.-J. Stock and A. Zepka “Model based hybrid proximity effect correction scheme combining dose modulation and shape adjustments,” J. Vac. Sci. Technol. B **29**, 06F315 (2011).
20. L. E. Ocola, “Nanoscale geometry assisted proximity effect correction for electron beam direct write nanolithography,” J. Vac. Sci. Technol. B **27**(6), 2569 (2009).
21. F. Yesilkoy, C. Kwangsik, M. Dagenais, and M. Peckerar, “Implementation of E-Beam Proximity Effect Correction using linear programming techniques for the fabrication of asymmetric bow-tie antennas,” Solid-State Electron. **54**(10), 1211–1215 (2010).
22. R. Patil, S. Lan, and A. V. Gopal, “Fabrication of large-area two-dimensional array of air holes with different hole shapes for optical and terahertz wavelength regions,” J. Nanophotonics **8**(1), 083896 (2014).
23. L. Allen, S. M. Barrnet, and M. J. Padgett, *Optical Angular Momentum* (Taylor and Francis Group 2003).
24. L. Marrucci, C. Manzo, and D. Paparo, “Optical Spin-to-Orbital Angular Momentum Conversion in Inhomogeneous Anisotropic Media,” Phys. Rev. Lett. **96**(16), 163905 (2006).
25. L. Marruci, E. Karimi, S. Slussarenko, B. Piccirillo, E. Santamato, E. Nagali, and F. Sciarrino, “Spin-to-orbital conversion of the angular momentum of light and its classical and quantum applications,” J. Opt. **13**(6), 064001 (2011).
26. The error given here is the standard error of the mean, defined as the standard deviation over the square root of the sample size, i.e. $\sigma/\sqrt{N}$.
27. R. Wüest, P. Strasser, M. Jungo, F. Robin, D. Erni, and H. Jäcke, “An efficient proximity-effect correction method for electron-beam patterning of photonic-crystal devices,” Microelectron. Eng. **67-68**, 182–188 (2003).
28. C. Enkrich, M. Wegener, S. Linden, S. Burger, L. Zschiedrich, F. Schmidt, J. F. Zhou, T. Koschny, and C. M. Soukoulis, “Magnetic Metamaterials at Telecommunication and Visible Frequencies,” Phys. Rev. Lett. **95**(20), 203901 (2005).
29. M. Husnik, M. W. Klain, N. Feth, M. König, J. Niegemann, K. Busch, S. Linden, and M. Wegener, “Absolute extinction cross-section of individual magnetic split-ring resonators,” Nat. Photonics **2**(10), 614–617 (2008).

1. Introduction

Metamaterials and their two-dimensional equivalent, metasurfaces, promise novel optical effects [1–3], as well as flat and miniaturized versions of bulk optical components [4–6], such as flat lenses [7], Pancharatnam-Berry phase optical elements [8–10], holographic gratings [8,11] or spiral phase plates [1]. However, in many cases the efficiency of such devices is too low for realistic applications. The performance - measured by how effectively light is converted by the metasurface into the desired mode - is limited for a variety of reasons: material losses, sub-optimal structure design and limitations of fabrication technology. This necessitates further work to improve device performance, which can be achieved in a variety of ways. For example, improved antenna design [12], low-loss constituent materials [13], improved material quality [14] or improved device fabrication. In this letter we address the effect of fabrication procedures on device performance. As a demonstrative metasurface we use a plasmonic *q*-plate [9,10], consisting of an angular dependent array of L-shaped nanoantennas, that generates optical orbital angular momentum through spin-to-orbit coupling. The converted light has orthogonal polarization to the unconverted light and hence we can accurately measure the optical performance of the device. We show that intra-structure proximity-error-correction (PEC) of the component nanoantennas increases both the fabrication fidelity and the optical performance of our devices. Furthermore, we find that the fabrication fidelity alone is not a good predictor of the optical performance of a device and therefore optical measurements are necessary when assessing fabrication quality. Our analysis is performed for an exemplary metasurface, yet the approach is general and applicable to metasurfaces with different constituent antennas and materials.

2. Proximity error and correction

The proximity error is caused during the lithography step of device fabrication. Here we focus on electron beam lithography and its associated proximity effect [15]. In a state-of-the art electron beam lithography system, the typical beam spot size is on the order of one nanometer on the top surface of the resist. However, under propagation through the resist and subsequent impact on the substrate, electrons are scattered and secondary electrons are generated, all of which contribute to the resist exposure. Thus, rather than exposing a spot with clear defined

#248011 Received 17 Aug 2015; revised 1 Oct 2015; accepted 26 Oct 2015; published 10 Nov 2015

edges, the exposed area resembles a fuzzy, airbrushed circle and the actual dose received during lithography depends not only on the direct exposure, but also on the shape and dose of nearby exposed areas [16]. Two length-scales are associated with the proximity effect. The first is associated with the generation of secondary electrons and extends over micrometers (depending on the lithography system and substrate) [16]. Due to the much smaller size of plasmonic components this does not affect the shape of an individual antenna, but can influence the uniformity across an array. The second length-scale, associated with a broadening of the electron beam during propagation through the resist, is on the order of 100 nm and impacts on the shape of an individual nanoantenna. It is this latter, intra-structure proximity effect, that we will consider in this work.

PEC [17] accounts for the effect of the proximity error during by adjusting the lithography design, either the exposed shape (shape-correction), the exposure dose distribution (dose-correction) or both. For our antenna arrays (see Fig. 1), the dimensions of the constituent L-shaped nanoantennas (approximately 200 nm arm length, 120 nm arm width, see Fig. 1(b) are comparable to the beam broadening (150 nm). Therefore, shape-correction provides a more controlled approach to PEC [18,19] and was chosen for this work. Small "serifs", either additions or cutouts, are added to the structure, see Fig. 1(c). Previous reports [19–22] have shown that this approach (and other intra-structure PEC) increases the fabrication fidelity, but they neglected to quantify the effect on the optical performance of the fabricated device, relying on scanning electron microscope images alone to judge device quality.

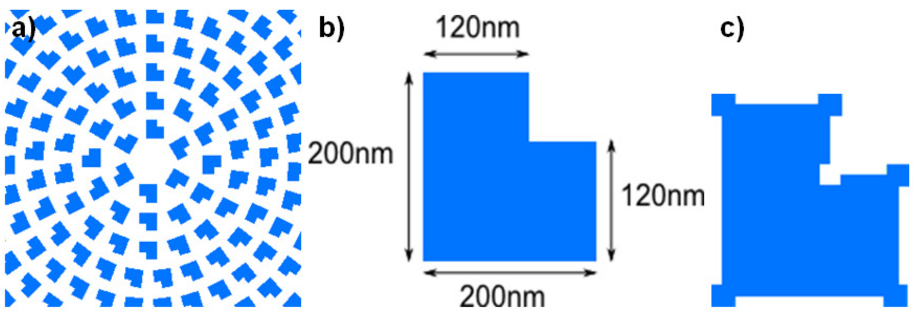

Fig. 1. Schematics taken from the electron beam lithography design file of **a)** an antenna array, **b)** and individual nanoantenna without PEC and **c)** a nanoantenna with shape-correction PEC (each little square has 20nm sidelength).

3. Experiment and results

We assess both the fabrication and measurement fidelity of a range of plasmonic q-plates [9,10], acting as an exemplary metasurface. A q-plate is a Pancharatnam-Berry phase optical element, which converts spin-angular-momentum to optical-angular-momentum (OAM) [23] for light, with the exact value of OAM (which is $\ell\hbar$ per photon), depending on both the geometry of the q-plate and the incident polarization [24,25]. All devices investigated have the same device area (a circle with 100 µm diameter) and geometry. Consequently they impart the same value of OAM upon spin-to-orbit conversion (in our case $\ell = 2$).

Multiple q-plates were fabricated, with a range of target dimensions for the constituent nanoantennas (200-220 nm arm length and 120-140 nm arm width) and both with and without PEC. Arrays with various sizes of the additions/cutouts (20nm, 40nm and 60nm) were investigated. Results showed that only the smallest variation (20nm) can be modeled as a perturbation of the ideal antenna, the other values showed fundamentally different antenna behaviour, and therefore only these 20nm additions/cutouts are suitable for PEC (with our given antenna dimensions) and will be considered for the remainder of this paper. All devices were fabricated on a single substrate, ensuring that the PEC and target dimensions were the only variation between devices, keeping other potential sources of fabrication error, e.g. film

#248011 Received 17 Aug 2015; revised 1 Oct 2015; accepted 26 Oct 2015; published 10 Nov 2015

thickness or quality, constant. Fabrication was performed through electron beam lithography (Raith Pioneer 30 kV e-beam system) with a 300 nm thick bi-layer PMMA resist on a fused silica substrate. A transparent indium tin oxide (ITO) layer between the resist and the silica substrate ensures charge dissipation during the exposure and subsequent electron microscope imaging. The effect of the ITO layer on the optical performance of the antennas was included during device design [10]. A thin (80 nm) gold layer was deposited on the patterned resist using thermal evaporation, with a subsequent metal lift-off step.

The fabrication fidelity is defined as the average overlap between fabricated nanoantennas within one array and an ideally shaped nanoantenna with dimensions identical to the average dimensions for this array. These average dimensions were obtained, by averaging the size and width of each antenna arm for 20 to 25 antennas per array. The size information was obtained from image analysis using the image evaluation software FIJI, which was also used to evaluate the overlap between the actual and ideal antenna. These average dimensions present a better reference than the target dimension, as many factors impact the fabricated antenna size, such as run-to-run variations in the resists thickness or fluctuations in electron beam current. Therefore there is always a deviation between the target and actual dimensions of nanophotonic and plasmonic devices, independent of the impact of PEC. In order to decouple the effects of these variations from the effect of PEC, the average dimensions of each array are used as a reference. The measurement fidelity is the ratio of the experimentally measured optical performance over the theoretical values for the same antenna dimensions. In the case of the q-plate, the optical performance is given by the purity of the transmitted beam, which is the percentage of light propagating through the q-plate that is converted, i.e given OAM, and was measured using the same set-up as in references [9,10], with theoretical values obtained from 3D FDTD simulations (1nm mesh). Separate simulations were performed for each array, using the average dimensions of that array, to decouple the effect of PEC from other variations during fabrication, as was the case for the fabrication fidelity.

3.1 Fabrication fidelity

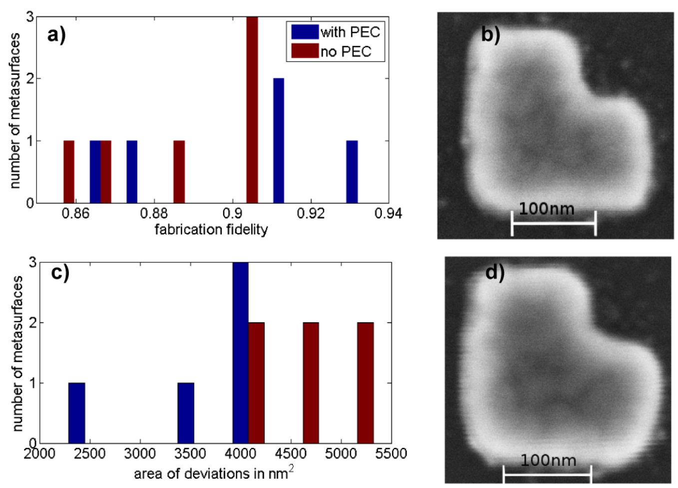

Fig. 2. **a)** and **c)** Histograms of the fabrication fidelity and the area of deviations, respectively. **b)** and **d)** Scanning electron microscope images of a representative nanoantenna with (**b**) and without (**d**) PEC.

We first assess the fabrication fidelity for metasurfaces with and without PEC, shown in Fig. 2(a). Those arrays with PEC show a higher average fabrication fidelity (90.2 ± 1.3%) than those without (88.6 ± 0.8%) [26]. The improvement is small, as the initial devices already have high fabrication fidelity, as illustrated in Fig. 2(b) and (d), which show that it is difficult to reliably differentiate between a structure with (b) and without PEC (d). While this

#248011 Received 17 Aug 2015; revised 1 Oct 2015; accepted 26 Oct 2015; published 10 Nov 2015

improvement in the fabrication fidelity seems small, it does represent a significant reduction of the “defect” area - the total area over which a fabricated and an ideal antenna differ, as shown in Fig. 2(b).

3.2 Measurement fidelity

While the small improvement in the fabrication fidelity reported above is promising, the effect of PEC on the optical performance of our metasurfaces is far more important. Simulations of arrays with ideally-shaped nanoantennas predict purities as high as 60% for the wavelength range under consideration (760-790 nm). In Fig. 3 we show the measurement fidelity, which in our case is the experimentally observed purity over the theoretical purity for an ideal device (see section 3), for devices with and without PEC, as a function of the fabrication fidelity and the defect area. There is no correlation ($R^2 = 0.0$) between the measurement and fabrication fidelity and we can only observe weak correlation ($R^2 = 0.1$) between the measurement fidelity and the defect area, with a reduced defect area resulting in an increased measurement fidelity. Most notably, our results show that the PEC provides a clear improvement, from an average measurement fidelity of 73.3 ± 3% without PEC to 83.1 ± 3% with PEC [26]. We attribute the remaining discrepancy to a range of potential sources, such as a non-ideal vertical profile, non-textbook values of our metal parameters (e.g. conductivity and absorption) and the fact that the fabrication fidelity is still not perfect.

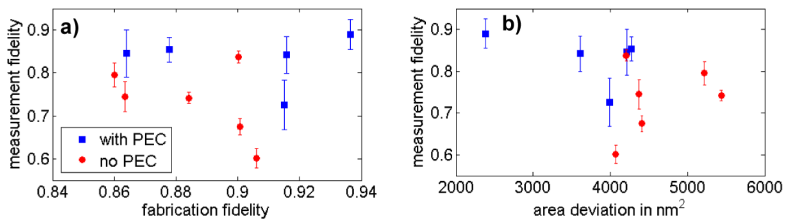

Fig. 3. Measurement fidelity vs **a)** the fabrication fidelity and **b)** the defect area.

4. Discussion

In the above analysis we seem to have non intuitive results: fabrication and measurement fidelity lack clear correlation and structures with PEC outperform those without PEC for the same fabrication fidelity. However, as we will outline below, these results are in line with the general understanding of plasmonic antennas and show the danger of directly linking structure measurements (the fabrication fidelity) to effects dependent on the behaviour of plasmonic resonances (the measurement fidelity).

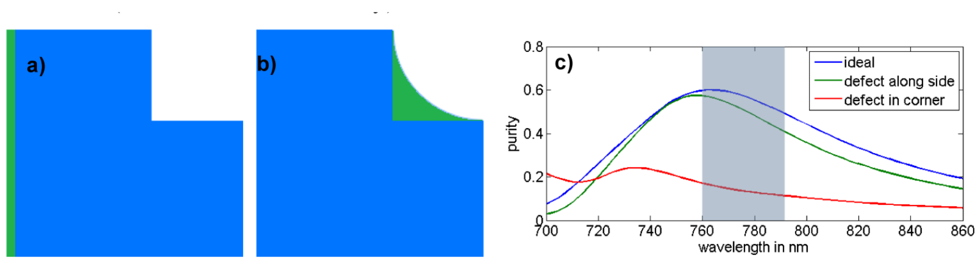

Fig. 4. **a)** and **b)**, sketch (to scale) of L-antennas with the same fabrication fidelity, but the deviating area (green region) concentrated along one arm (**a**) or in one corner (**b**) respectively. **c)** Purity for the two antennas compared to the ideal nanoantenna with same dimensions, the gray shaded region indicates the wavelength range used during experiments.

The definition of the fabrication fidelity gives equal weight to all deviations from the ideal shape, independent of their physical location. However, the plasmonic behaviour is affected differently by deviations at different physical locations, since plasmonic resonances depend

#248011 Received 17 Aug 2015; revised 1 Oct 2015; accepted 26 Oct 2015; published 10 Nov 2015

critically on the shape of the nanoantenna. A slight bulge out along the complete length of an arm can have a similar area deviation as strong rounding of a corner - and therefore the same fabrication fidelity - but could have a much smaller effect on the plasmonic resonances and therefore the optical behaviour. For example, the two antennas sketched in Fig. 4 represent exactly this case, they have the same fabrication fidelity (95.8%), but as explained in the previous sentence, the location of the defect matters. In the case where the deviations are along the length of an arm, the optical performance drops slightly (89.6 ± 1.3% average measurement fidelity over shaded area), while the second antenna, with deviations concentrated in the inner corner has a strikingly different optical behaviour (24.7 ± 0.6% average measurement fidelity) [26]. Shape-correction PEC is specifically designed to increase the sharpness of corners and will therefore better reduce deviations at these corners compared to other areas of the antenna. By correcting the shape of the antenna where it matters most, the PEC improves measurement fidelity much more than fabrication fidelity.

5 Conclusions

In summary we have shown an increase in fabrication fidelity for PEC nanoantennas, through a significant reduction in the defect area. Metasurfaces constructed of these PEC antennas showed strongly improved optical performance, demonstrated here by an increased measurement fidelity (average of 83%) of a plasmonic *q*-plate. The lack of correlation between measurement and fabrication fidelity demonstrates that the fabrication fidelity alone cannot be used as an accurate indicator of optical device performance and does not present a good measure of fabrication quality. It is therefore necessary to perform optical measurements when assessing the impact of changes to fabrication procedures, such as the implementation of PEC.

The significant improvements to the device performance provided by the shape-correction, intra-structure PEC should be applicable to any structure with dimensions comparable to the beam broadening in the resist during lithography, just as inter-structure PEC has done for other optical devices [27] without any additional fabrication steps. Due to the field distribution within such structures, the effect is particularly pronounced, and therefore important, for devices with sharp corners - the L-shaped antennas investigated here, but also other antenna designs such as V- or Y-shaped antennas and split ring resonators [3,28,29].

Acknowledgments

This work was funded by the Canada Excellence Research Chair (CERC) initiative.